

FEDSM98-5022

**NUMERICAL PREDICTION OF PARTICLE DISPERSION IN A MIXING LAYER
USING AN EULERIAN TWO-PHASE FLOW MODEL**

Paulo J. Oliveira

Departamento de Engenharia Electromecânica
Universidade da Beira Interior
6200 Covilhã, Portugal

Raad I. Issa

Department of Mechanical Engineering
Imperial College of Science, Technology and Medicine
London SW7 2BX, UK

ABSTRACT

The paper describes the application of a numerical method to the prediction of dispersion of heavy particles in a shear layer. The method solves the Eulerian, two-fluid model averaged equations and caters for turbulence in the continuous phase by an extension of the $k-\epsilon$ model. Turbulence-related quantities of the dispersed phase are obtained from the corresponding continuous phase values through response functions and these are based on the recent work of Wang and Stock (1993). The results are in reasonable agreement with available detailed measurements, even though the $k-\epsilon$ model is known to be inadequate to represent the unsteady behaviour of the large vortices in the layer. Particle dispersion is well predicted when the Stokes number is greater than unity and is underpredicted when it is around unity.

1. INTRODUCTION

Two-phase flows involving solid particles carried by a gas stream are common in many engineering applications and it is thus important for the practicing engineer to have means to predict their relevant characteristics. These required flow characteristics are typically the mean velocities of each phase, the gas and the particles, and the concentration of the particulate phase which will indicate how the particles are distributed. It is now known that some of these type of flows can be very complex in the details and the mechanisms by which particles respond to the fluid turbulence; the reviews by Eaton and Fessler (1994) and Crowe et al. (1996) clearly demonstrate that particles are dispersed in a non-homogeneous way, even in homogeneous turbulence, and tend to concentrate in regions of low instantaneous vorticity thus responding to the large-scale coherent structures in the turbulent motions. Such

type of behaviour can only be predicted by sophisticated simulation methods, like direct-numerical simulations and large-eddy simulation, or by methods which use transport equations for the many fluid/particle correlations (e.g., Simonin et al 1993). However for engineering applications, results from simpler models, typically based on extensions to two-phase flows of the well-known two-equation turbulence models used in single-phase flows, may be sufficient for the purpose.

The authors have been developing a model of this type, which has been applied with some success to confined jets (Issa and Oliveira 1995) and phase-fraction mixing layers (Issa and Oliveira 1996). The purpose here is, first, to introduce a different response model and, secondly, to apply the method to the prediction of particle dispersion in a velocity mixing layer problem for which detailed experimental data are available.

The method in question solves the Eulerian, two-fluid model equations which are composed of the ensemble-averaged momentum and continuity equations for each phase in conjunction with transport equations for k and ϵ which are used to characterize the effects of turbulence. The equations are discretised using a finite-volume technique and the resulting equations are solved in an iterative algorithm which is based on the pressure-correction scheme.

Central to the two-phase model used, in particular the model for the effects of turbulence, is the assumption of simple algebraic relations between the local turbulence quantities of the continuous and dispersed phases. This assumption then facilitates the correlation between the turbulent stresses for the dispersed phase and those of the continuous phase which in turn are related by an eddy viscosity to the rates of strain in that phase. The above assumption requires the prescription of response functions correlating the turbulence energies (C_k), the turbulent diffusivities (C_ν) and the velocity correlations (C_i).

These functions are obtained from the analysis of Wang and Stock (1993) which duly accounts (at least in isotropic turbulence) for the three known effects: crossing-trajectories (reduced dispersion with increased drift velocity), continuity (higher dispersion in the direction of the drift than in other directions), and inertia (stronger particle velocity-correlations with increase in particle size).

The method incorporating these new response functions has been successfully applied to the problem of dispersion of heavy particles in a confined air jet and the results have been reported elsewhere (Issa and Oliveira, 1997). In the present paper, the dispersion of solid particles in a mixing layer is computed and the predictions are compared with the data of Hishida et. al. (1992). The effect of particle inertia on the response functions will be assessed from the results for the 3 particle sizes used in the experiments. Likewise, the effect of crossing trajectories is assessed from a comparison between cases where the bulk velocity, and thus the mean drift, was varied in experiments performed by the same group (reported in Ishima et al. 1993)

2. EQUATIONS AND BASIC TURBULENCE CLOSURES

The phase-averaged continuity and momentum equations for each phase are given by (e.g. Issa and Oliveira 1995, 1997):

$$\nabla \cdot (\bar{\alpha}_k \rho_k \tilde{\mathbf{u}}_k) = 0 \quad (1)$$

and

$$\begin{aligned} \frac{\partial}{\partial t} (\bar{\alpha}_k \rho_k \tilde{\mathbf{u}}_k) + \nabla \cdot (\bar{\alpha}_k \rho_k \tilde{\mathbf{u}}_k \otimes \tilde{\mathbf{u}}_k) = - \bar{\alpha}_k \nabla \tilde{p} \\ + \bar{\alpha}_k \nabla \cdot \tilde{\tau}_k + \nabla \cdot \bar{\alpha}_k \tilde{\tau}_k^t + \rho_k \bar{\alpha}_k \mathbf{g} + \overline{\mathbf{F}_{D_k}} \end{aligned} \quad (2)$$

where $\bar{\alpha}_k$ denotes the time-average volume fraction of phase k , with index k taking the value $k = g$ for the gas phase (air) and $k = p$ for the particulate phase. Both the molecular $\tilde{\tau}_k$ and the turbulent $\tilde{\tau}_k^t$ stress tensors are assumed to follow Newtonian constitutive laws, as explained below. The main dependent variables in the above equations, besides the volume fractions, are the average pressure \tilde{p} and the phase averaged velocities defined by:

$$\tilde{\mathbf{u}}_k = \frac{\overline{\alpha_k \mathbf{u}_k}}{\bar{\alpha}_k} \quad (3)$$

which should be distinguished from the usual time-averaged velocity $\bar{\mathbf{u}}_k$, with an overbar denoting a time average.

If the particulate phase is assumed to be formed by many spherical particles, all with the same diameter d_p , then the

interaction term in (2) is due solely to interphase drag, since the density ratio is high $\rho_p/\rho_g \gg 1$, and is given by (Issa and Oliveira 1995):

$$\begin{aligned} \overline{\mathbf{F}_{D_g}} = C_f \bar{\alpha}_p \bar{\alpha}_g (\bar{\mathbf{u}}_p - \bar{\mathbf{u}}_g) \\ = C_f \left(\bar{\alpha}_p \bar{\alpha}_g (\tilde{\mathbf{u}}_p - \tilde{\mathbf{u}}_g) + (\bar{\alpha}_g \eta_p + \bar{\alpha}_p \eta_g) \nabla \bar{\alpha}_p \right) \end{aligned} \quad (4)$$

where $C_f \equiv 18\mu_g f(\text{Re}_p)/d_p^2$ is a standard drag coefficient for which $f(\text{Re}_p) = 1 + 0.15\text{Re}_p^{0.687}$ ($\text{Re}_p \equiv \rho_g \bar{\mathbf{u}}_r d_p / \mu_g$), and η_k are eddy diffusivities defined below. In (4), the second equality results from substitution of the time-average velocities by $\bar{\mathbf{u}}_k = \tilde{\mathbf{u}}_k + \overline{\mathbf{u}_k'} = \tilde{\mathbf{u}}_k - \overline{\alpha_k \mathbf{u}_k' / \bar{\alpha}_k}$, based on the definition of the two averages, and from the gradient diffusion hypothesis for the transport of α by turbulent fluctuations, that is $\overline{\alpha_k \mathbf{u}_k'} = -\eta_k \nabla \bar{\alpha}_k$. The turbulent diffusivity of the k -phase, η_k , is related to the eddy viscosity μ_g^t (with $\nu_g^t = \mu_g^t / \rho_g$) through the algebraic model explained in the next section, while the latter is obtained from an extension of the two-equation k - ϵ turbulence model (see Issa and Oliveira 1997 for details). Thus:

$$\tilde{\tau}_k^t = \mu_k^t (\nabla \bar{\mathbf{u}}_k + \nabla \bar{\mathbf{u}}_k^T) - \frac{2}{3} (\mu_k^t \nabla \cdot \bar{\mathbf{u}}_k + \rho_k \bar{\mathbf{k}}_k) \delta \quad (5)$$

$$\begin{aligned} \frac{\partial}{\partial t} (\bar{\alpha}_g \rho_g \tilde{\mathbf{k}}_g) + \nabla \cdot (\bar{\alpha}_g \rho_g \tilde{\mathbf{u}}_g \tilde{\mathbf{k}}_g) \\ = \nabla \cdot (\bar{\alpha}_g \frac{\mu_g^t}{\sigma_k} \nabla \tilde{\mathbf{k}}_g) + \bar{\alpha}_g (G - \rho_g \tilde{\epsilon}_g) + S_p^k \end{aligned} \quad (6)$$

$$\begin{aligned} \frac{\partial}{\partial t} (\bar{\alpha}_g \rho_g \tilde{\epsilon}_g) + \nabla \cdot (\bar{\alpha}_g \rho_g \tilde{\mathbf{u}}_g \tilde{\epsilon}_g) \\ = \nabla \cdot (\bar{\alpha}_g \frac{\mu_g^t}{\sigma_\epsilon} \nabla \tilde{\epsilon}_g) + \bar{\alpha}_g \frac{\tilde{\epsilon}_g}{k_g} (C_1 G - C_2 \rho_g \tilde{\epsilon}_g) + S_p^\epsilon \end{aligned} \quad (7)$$

and

$$\mu_g^t = \rho_g C_\mu \frac{\tilde{\mathbf{k}}_g^2}{\tilde{\epsilon}_g} \quad \text{and} \quad G = \mu_g^t \nabla \bar{\mathbf{u}}_g : (\nabla \bar{\mathbf{u}}_g + \nabla \bar{\mathbf{u}}_g^T). \quad (8)$$

Standard values are assigned to the k - ϵ model constants ($C_1 = 1.44$, $C_2 = 1.92$, $C_\mu = 0.09$, $\sigma_k = 1.0$, $\sigma_\epsilon = 1.22$). In the transport equations for the turbulent kinetic energy of the gas phase $\tilde{\mathbf{k}}_g$ (Eq. 6) and its dissipation rate $\tilde{\epsilon}_g$ (Eq. 7), terms S_p^k and S_p^ϵ arise from correlations between the drag force and velocity fluctuations and are given by (see Issa and Oliveira 1996):

$$\begin{aligned} S_p^k = -C_f \left(\eta_g \nabla \bar{\alpha}_p \cdot \bar{\mathbf{u}}_r + 2 \bar{\alpha}_g \bar{\alpha}_p \tilde{\mathbf{k}}_g (1 - C_i) \right. \\ \left. - \eta_g (\eta_g - \eta_p) \nabla \bar{\alpha}_p \cdot \nabla \bar{\alpha}_p \right) \end{aligned} \quad (9)$$

$$S_p^\epsilon = -C_3 \frac{\tilde{\epsilon}_g}{\tilde{k}_g} 2C_f \bar{\alpha}_g \bar{\alpha}_p \tilde{k}_g (1 - C_i). \quad (10)$$

where constant $C_3 = 1$, \bar{u}_r is the mean slip velocity and C_i is given in the next section.

3. RESPONSE FUNCTIONS

Some dispersion-related characteristics of the particulate phase appear in the above equations which need to be related to other variables; namely, the eddy viscosity $\nu_p^t = \mu_p^t / \rho_p$, turbulent diffusivity η_p , turbulent kinetic energy \tilde{k}_p and mixed velocity correlation $\overline{\mathbf{u}_p' \cdot \mathbf{u}_g'}$. This closure problem is addressed via algebraic relations from which the response functions:

$$C_\nu \equiv \nu_p^t / \nu_g^t \quad (11)$$

$$C_\eta \equiv \eta_p / \eta_o \quad (12)$$

$$C_k \equiv \tilde{k}_p / \tilde{k}_g, \quad (13)$$

$$C_i \equiv \frac{1}{2} \overline{\mathbf{u}_p' \cdot \mathbf{u}_g'} / \tilde{k}_g, \quad (14)$$

can be obtained. In Eq. (12), η_o is the diffusivity of a tracer in the gas phase, given by $\eta_o = \nu_g^t / \sigma_o$ where σ_o is a Schmidt number. Wang and Stock (1993) have analysed the response of particles to isotropic homogeneous turbulence with view to obtaining explicit algebraic expressions for the dispersion coefficient and correlation functions. The purpose was thus similar to that in previous work by Reeks (1977) and Pismen and Nir (1978), but some additional assumptions made by Wang and Stock lead to simplification of the ensuing analysis and the final expressions were in closed form and much simpler than the obtained by the other authors. In Issa and Oliveira (1997) it is shown how the analysis of Wang and Stock can be used to give all the required response functions:

$$C_\nu = C_\eta \quad (15)$$

$$C_{\eta,x} = \frac{1}{D} \frac{T}{T_E} \frac{1}{\beta} \quad \text{and} \quad C_{\eta,y} = \frac{1-0.5m_T\gamma/D}{D} \frac{T}{T_E} \frac{1}{\beta} \quad (16)$$

$$C_{k,x} = \frac{1}{1+St_TD} \quad \text{and} \quad C_{k,y} = \frac{1+St_T(D-0.5\gamma m_T)}{(1+St_TD)^2} \quad (17)$$

$$C_i = C_k \quad (18)$$

where $D \equiv \sqrt{(1 + (m_T\gamma)^2)}$, the Stokes numbers are defined as $St \equiv t_p/T_E$ or $St_T \equiv t_p/T$ with the time scales defined below, the crossing-trajectories parameter is defined as $\gamma \equiv \bar{u}_r / u_g'$ and the turbulence structure parameter as $m \equiv T_E/t_e$ or $m_T \equiv m(T/T_E)$. It is noted that the response functions can

have two values, in the direction of the mean drift (here denoted with index x) and perpendicularly to it (index y); so, for example C_k can take the value $C_{k,x}$ (which relates the streamwise rms velocity fluctuation of the particles to that of the gas phase) or $C_{k,y}$ (similar for the lateral velocity fluctuations). In a 3-D situation, z -components of the response functions would be equal to the y -components above. The time scales appearing in all these expressions are: t_p , particle relaxation time scale, T_E , Eulerian fluid integral time scale in a frame moving with the mean fluid velocity, t_e , time scale of the energy containing eddies, T_L , Lagrangian integral time scale, T , fluid integral time scale seen by a particle with zero drift velocity. In this study we take $T_L = 0.41 k/\epsilon$ (Calabrese and Middleman, 1979), $T_E = T_L/\beta$ with $\beta = 0.356$ (Wang and Stock), $t_e = T_E/m$ with $m = 1$, T/T_E is given by an empirical function of St in Wang and Stock, and $t_p = \rho_p d_p^2 / 18\mu_g f(Re_p)$.

4. NUMERICAL METHOD

The differential equations are integrated over each cell of the computational mesh using a finite-volume discretisation applied in a collocated arrangement — all variables are stored at the centre of the cell. The outcome of the discretisation is a number of sets of algebraic linearised equations, one for each dependent variable. These are solved sequentially, by means of conjugate-gradient type solvers, and a pressure-correction technique is utilized in order to obtain a pressure field which forces the sum of the velocity fields of the two phases to satisfy an overall continuity constraint. The particulate phase volume-fraction results from the solution of the continuity equation of this phase treated as a transport equation for $\bar{\alpha}_p$. Details of the two-phase flow algorithm can be found in Issa and Oliveira (1994).

Strong coupling between the momentum equations of the two phases, arising from large drag forces, can be dealt with by the partial elimination algorithm described in Oliveira and Issa (1994).

No use is made of any under-relaxation factor and numerical stability is controlled by reducing the time-step used in the pseudo time advancement technique adopted. This is why the time-dependent terms were retained in the momentum equations (2), and also in the k - and ϵ -equations (6-7), even if interest here is confined to the final steady state solution. For the present calculations, the time-step was set to $\delta t = 10^{-6}$ s (yielding a small local Courant number of about 3×10^{-3} on the fine mesh) during the first 1000 time steps, and was then increased to $\delta t = 10^{-4}$ s for the subsequent time advancement and for all the other runs, which used the first solution as the initial field. This procedure was found to work well and was required to cope with the numerical stability problems associated with very large velocity gradients in the

interface region between the two velocity layers which induced very large turbulence production and dissipation.

5. RESULTS

The problem considered is the plane mixing-layer, two-phase flow reported by Hishida et al. (1992) and Ishima et al. (1993). Two separated layers of air with different uniform velocities ($U_1 = 4$ m/s and $U_2 = 13$ m/s) are allowed to mix at the trailing edge of two splitter plates, the point defining the origin of the mixing layer. Solid particles with three different sizes ($d_p = 42, 72$ and $135 \mu\text{m}$; $\rho_p = 2590 \text{ kg/m}^3$) were injected there, through a 0.57 mm gap in-between the two 0.3mm -thick plates, and with a velocity approximately equal to $U_p = 1 \text{ m/s}$. The developing section and computational domain is a channel with half-width $H = 75 \text{ mm}$ and length $L = 450 \text{ mm}$ oriented vertically downwards along the x -direction. The computational meshes were generated in such a way that cells were concentrated along the dividing line ($y = 0$) where the gradients are expected to be highest. The boundary conditions are as follows: given inlet profiles at $x = 0$; no-slip conditions at the walls $y = \pm H$, a region devoid of particles; and vanishing streamwise gradients ($\partial/\partial x = 0$) for all quantities at the outlet $x = L$. The precise inlet conditions were difficult to assess from the data reported by the experimenters; it has been decided for the base inlet conditions to impose the two uniform velocities given above for the gas phase, a particle velocity of about 1 m/s at the splitter plate opening (which could be resolved by the fine mesh with 6-7 cells) and a void-fraction of around 10^{-5} . This value is consistent with the particle mass fluxes reported in Ishima et al (1993) and it is sufficiently low to ensure that the gas phase is barely affected by the presence of the particles, as often stated by the experimental authors. Their measurements of the particle number density N_d , based on Laser-Doppler burst counting, enables only an evaluation of a relative void-fraction - normalised by the maximum value at the station $x = 100 \text{ mm}$. Some variations on the imposed inlet conditions will also be considered below.

Fig. 1 shows profiles of the mean streamwise velocity of the gas phase at the measuring stations. Predictions are represented by lines and the experimental data by marks (an uncertainty of $\pm 5.4\%$ in mentioned by the authors). Three different meshes have been used: mesh-1 is a medium mesh (50×60 ; $\delta x_{\min} = 4 \text{ mm}$ and $\delta y_{\min} = 1 \text{ mm}$), which was then refined along y to obtain mesh-2 (50×100 , $\delta y_{\min} = 0.16 \text{ mm}$) and along x to obtain mesh-3 (80×60 , $\delta x_{\min} = 1 \text{ mm}$). It is clear from the figure that the numerical results obtained with these 3 meshes are hardly separable, thus demonstrating mesh independence, and mesh-2 was therefore adopted for the remaining predictions.

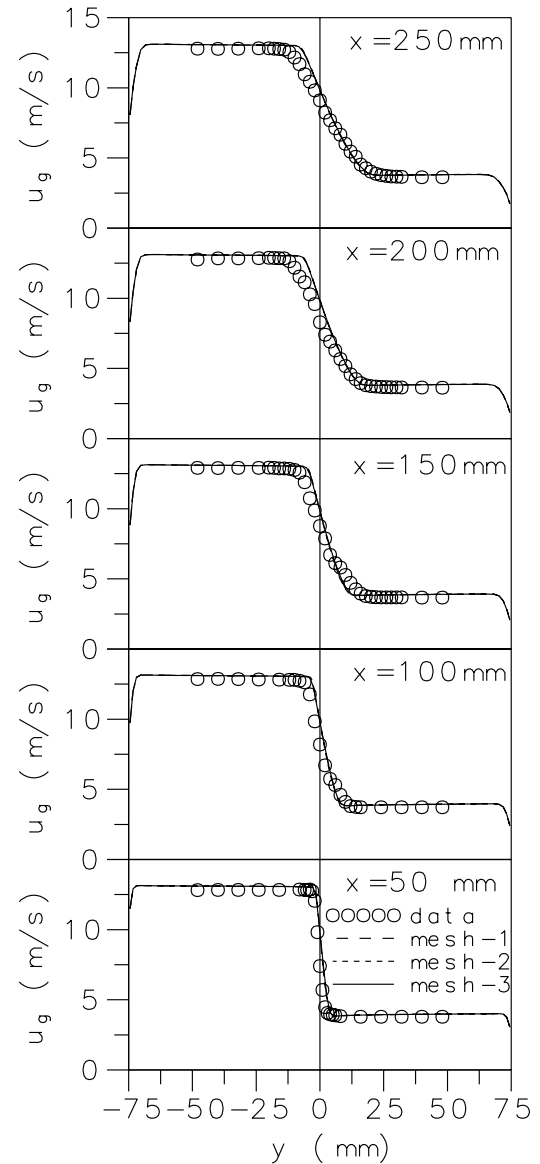


Fig. 1 Streamwise mean velocity component of the gas phase at different stations.
(marks: experiments; lines: simulations)

It is also seen that the $k-\epsilon$ model is able to resolve fairly well the step velocity profile, although the predictions on the high-velocity side seem to deviate slightly from the data thereby underpredicting the rate of spread (the experimental velocity diffuses faster than the predictions).

In fact the spread of the mixing layer, as measured by the axial variation of the half-velocity width, $b \equiv y(U_{0.75}) - y(U_{0.25})$, is seen in Fig. 2 to follow a straight line below the data. The case with a higher bulk velocity $U_b = 13 \text{ m/s}$ (for $U_2 = 21$ and $U_1 = 13 \text{ m/s}$; $U_b \equiv 0.5(U_2 + U_1)$) reported by

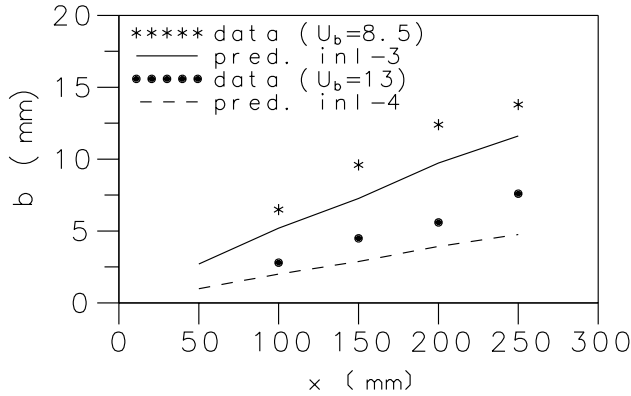


Fig. 2 Variation of the velocity mixing layer half-width with downstream distance.

Ishima et al is also plotted and shows the same trend. This feature is certainly a consequence of the shape of the turbulence intensity profiles predicted by the $k-\epsilon$ model in this mixing layer flow which are plotted against the data in Fig. 3 (uncertainty of the data is $\pm 6\%$). It is seen that the magnitude of the maxima, the shift of the curves towards the lower-velocity side of the layer and the general shape of the streamwise velocity fluctuations are well represented by the predictions, but the turbulence decay on the high-velocity side is much more gradual as shown by the data than the sharp predicted decrease. Unsteadiness, like intermittence and large-scale vortices in the mixing layer boundary, is responsible for that discrepancy as can be inferred from the large-eddy simulations of Chen (1994), for the same case, which show better agreement with the gradual decay of the velocity fluctuations in the data. The present steady formulation together with the $k-\epsilon$ model are obviously unsuited to represent that phenomena; nonetheless, the predictions are still in reasonable quantitative agreement.

As mentioned before, the gas phase fields are unaffected by the presence of the particles and so the above figures would be the same for any of the 3 particle size cases. The mean particle velocity is, however, strongly dependent on the diameter assumed for the particles, as shown in Fig. 4 where the predicted velocity profiles are compared with the experiments. There is fairly good agreement, especially in the central area where the concentration of particles is higher and also on the lower velocity side of the layer; the faster initial dispersion of the smaller particles followed by a progressive catching up by the larger ones, due to their weight, as indicated by the cross-over of the profiles after the station $x = 200$ mm, is seen in both the predictions and the experimental data. On the higher-velocity side, for $y \leq -5$ mm, the agreement is only qualitative for the lighter particles which are more affected by the structure of the turbulence

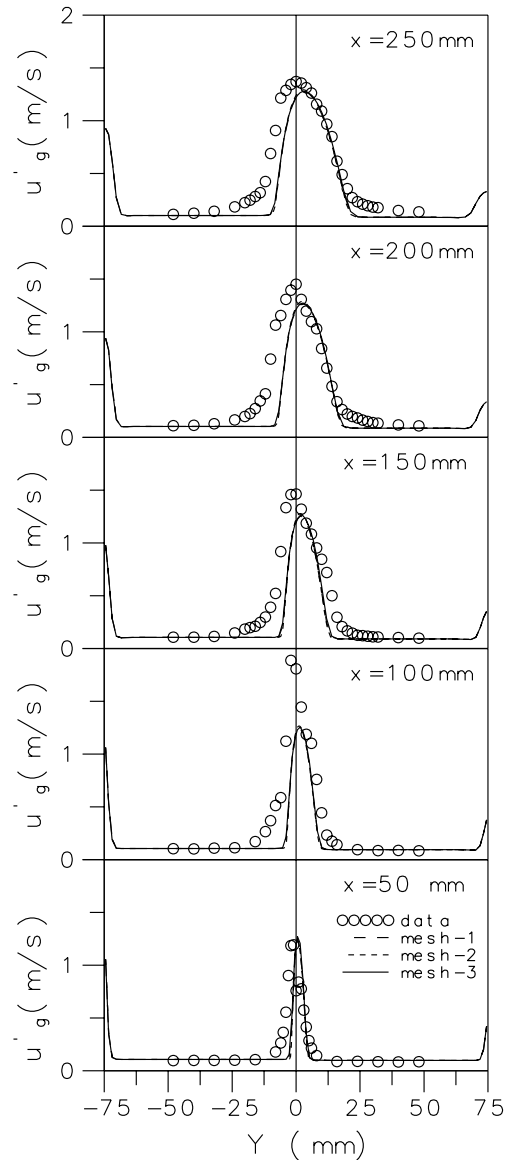


Fig. 3 Lateral profiles of the gas phase streamwise rms ($u' = (2k/3)^{1/2}$).

(large vortices). It should be borne in mind, while interpreting this figure, that the particle velocity has a finite value even when there are almost no particles present; so it is convenient to look simultaneously to a plot representing the particles concentration and realize that u_p has no meaning where $\bar{\alpha}_p \approx 0$.

Fig. 5 (a) presents the particle number density for the larger particle size ($d_p = 135 \mu\text{m}$), normalised by its maximum value at $x = 100$ mm in order to allow a comparison with the data given by the experimental authors. Fig. 5 (b) presents

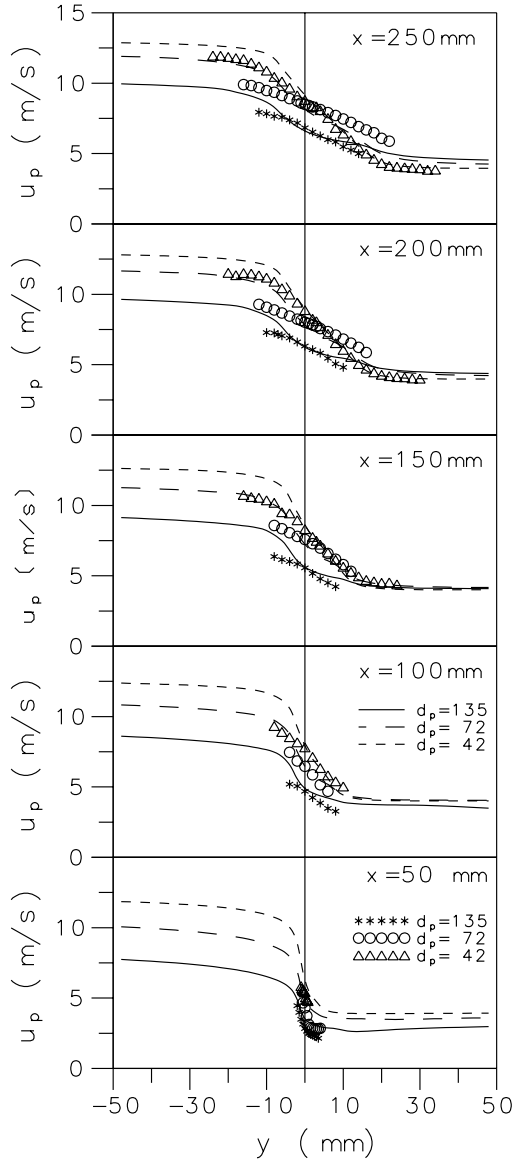
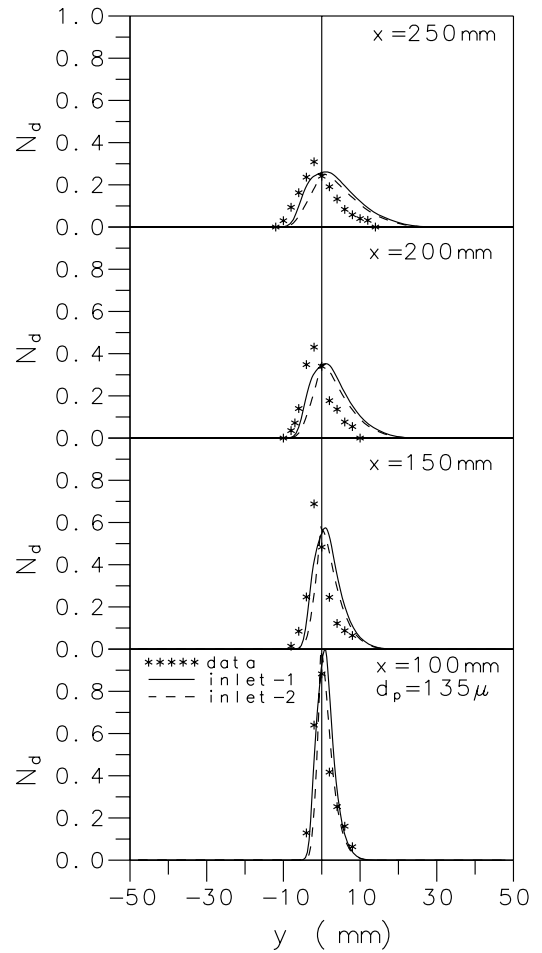


Fig. 4 Lateral profiles of the particle phase mean streamwise velocity component (lines: simulations; marks: experiments).

similar profiles for the medium particle size ($d_p = 72 \mu\text{m}$). It is noted here that the computations furnish the volume fraction from which the number density can be calculated via the relationship: $N_d = \bar{\alpha}_p / (\pi d_p^3 / 6)$; since the experiments only give a normalised value of N_d , it suffices to normalise in a similar way the volume fraction in order to have quantities which can be compared with each other.

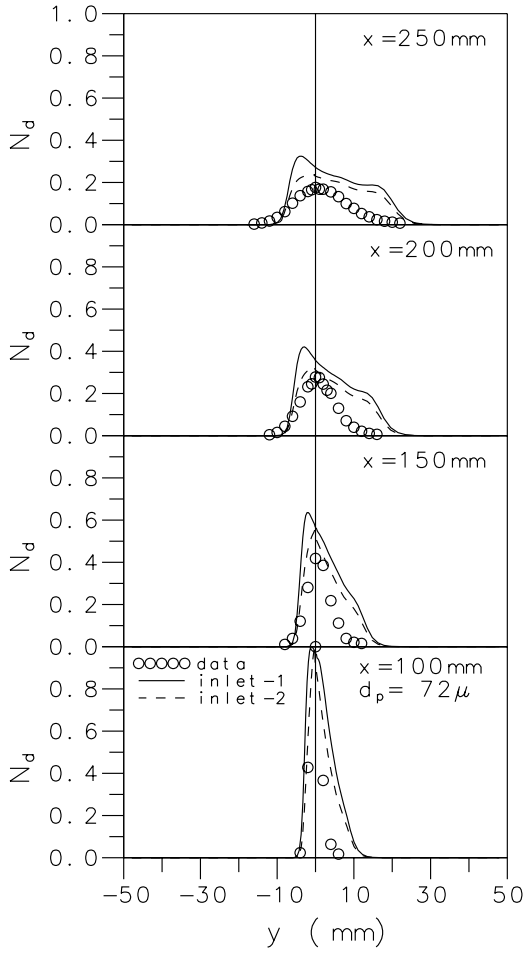
The dashed lines in Fig. 5 correspond to a slightly different inlet condition for the particulate phase: for inlet-2



(a) $d_p = 135 \mu\text{m}$

Fig. 5 Number density of the particles. Effect of different inlet conditions (marks: experiments; lines simulations).

the given profiles for $\bar{\alpha}_p$ and \tilde{u}_p are symmetric about the line $y = 0$ (whereas in inlet-1 they are somewhat asymmetric because the origin of the y -axis in the experiment was the trailing edge of the splitter plate on the high-velocity side) but have otherwise the same values as in condition inlet-1. Thus the figure enables one to assess the effect of a small variation in the inlet conditions (which, in any case, are not well known). It is seen that there is fair agreement between predictions and data, more so for the larger particles which are less affected by the structure of the turbulence (since $t_p/t_f > 1$ where t_f is some time scale for the coherent vortices in the mixing layer, typically defined as $\text{Cte} \times b / (U_2 - U_1)$) responding to it as in isotropic turbulence, the condition for which the response model of Wang and Stock was developed. Values for t_f are given by Hishida et al. (1992), cf. their figure 9, where it is seen that $t_p/t_f > 1$ for the $135 \mu\text{m}$ particles and



(b) $d_p = 72 \mu\text{m}$

Fig. 5 Number density of the particles. Effect of different inlet conditions (marks: experiments; lines simulations).

$t_p/t_f \approx 1$ for the small particles and also for the medium particles as they move further downstream. Since the ratio t_p/t_f controls the increased dispersion due to centrifuging by the coherent vortices (Crowe et al. 1996), an effect not accounted for by the present turbulence model, it comes as no surprise that dispersion is underpredicted for the $72 \mu\text{m}$ particles at the station $x = 250 \text{ mm}$ (Fig. 5 b). In the present model, the terms affecting particle dispersion (Issa and Oliveira 1995, 1996) are mainly the turbulent drag term (2nd term in the rhs of Eq. 4) and the normal Reynolds stress of the particulated phase, the $-\frac{2}{3}\rho_p \bar{k}_p$ term in Eq. (5), which in turn is governed by the C_k function (Eqs. 13 and 17).

The effect of a small change in the inlet conditions is appreciable, in this case the effect is stronger for the lighter

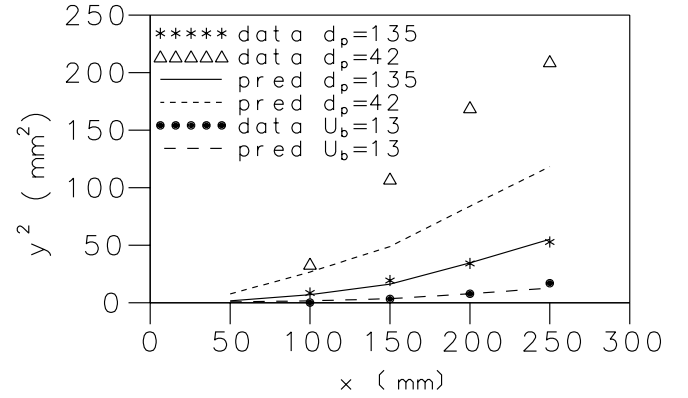


Fig. 6 Variation of the dispersion square displacement $\overline{y^2}$ with the downstream distance for 2 particle sizes and 2 bulk velocities.

particles (see Fig. 5 b) for which the predictions represented by the dashed line become closer to the data. This fact seems to indicate that without the precise knowledge of the particle phase inlet conditions it is difficult to obtain closer agreement between predictions and experiments than that shown in Figs. 5.

Since the motivation from the outset was to develop a prediction method able to give results useful for engineering applications, we turn attention to a variable which globally quantifies the dispersion. Fig. 6 shows the variation of the mean square displacement, computed as $\overline{y^2} \equiv \int \overline{\alpha_p} y^2 dy / \int \overline{\alpha_p} dy$ where the integrals are over the section of the channel, for the smallest and largest particles of the base case (for which $U_b = 8.5 \text{ m/s}$) and for the case with higher bulk velocity given in Ishima et al. ($U_b = 13 \text{ m/s}$, $d_p = 42 \mu\text{m}$). It is seen that the cases which are not dominated by the motion of the large vortices are very well predicted but dispersion of particles with small diameter in the base case is underpredicted. This situation worsens for particles that are further away from the mixing layer origin, when the typical large-scale vortices grow and their pairing-interaction intensifies.

6. SUMMARY AND CONCLUSIONS

A two-fluid model is applied to the computation of a plane mixing layer flow of air laden with solid particles. The model embodies “response functions” for the calculation of the particulate phase turbulent characteristics in terms of the corresponding air phase values which, in turn, are obtained from solution of transport equations for its turbulent kinetic energy and dissipation rate (two-phase flow $k-\epsilon$ model). A recent analysis of particle dispersion in isotropic turbulence by

Wang and Stock (1993) was used to derive all the required response functions.

The numerical predictions have been compared with the detailed experimental data of Hishida et al. (1992) and Ishima et al. (1993) who have measured the mean and fluctuating velocities of each phase and the particle number density for three particle sizes and two fluid bulk velocities. From the results it may be concluded that:

(i) Streamwise mean and rms velocity of the air phase are generally well predicted, except for the decay of k on the high-velocity side of the layer which is too abrupt compared with the gradual decay shown by the data. This deficiency can be attributed to the steady-state k - ϵ approach which fails to predict the effects of the large-scale vortical structures.

(ii) Predicted and measured mean axial velocities of the particulate phase are in qualitative agreement for all particle sizes and in quantitative agreement for the larger particles ($t_p/t_f > 1$). Results are better on the low-velocity side of the mixing layer. The faster initial dispersion of the lighter particles followed by acceleration of the heavier particles, due to their weight, are well predicted.

(iii) Particle concentration, as measured by its normalised number density, is predicted better for the heavier particles since these are the least responsive to the turbulence structure. The local variations of N_d for the particles with $d_p=72\mu\text{m}$ are not too bad compared with the data but the effect of the precise conditions assumed at inlet is important.

(iv) The growth of $\overline{y^2}$ (mean square displacement of particles, an overall measure of dispersion) is very well predicted for the large particles, and also for the small particles when the bulk velocity is higher – in both cases the effect of the turbulence structure on dispersion is reduced (see discussion in Ishima et al.). However, the rate of increase of $\overline{y^2}$ is greatly underpredicted for the small particles ($d_p=42\mu\text{m}$) in the base case ($U_b=8.5\text{ m/s}$) for the same reasons (in this case, $t_p/t_f \sim 1$ and the centrifuging effect of the large vortices dominates, see Eaton and Fessler 1994).

Acknowledgments

Financial support by JNICT-Portugal (Junta Nacional de Investigação Científica e Tecnológica) through project PBIC/CEG/2430/95 is gratefully acknowledged. The authors would like to thank Prof. M. Sommerfeld for providing the experimental data in tabulated form.

REFERENCES

Calabrese, R. V., and Middleman, S., 1979, "The Dispersion of Discrete Particles in a Turbulent Fluid Field", *AIChE. J.*, Vol. 25(6), pp. 1025-1035.

Chen, X-Q., 1994, "Numerical Simulation of Steady and Unsteady Two-Phase Spray Flows", Ph.D Thesis, IST, Technical Univ. of Lisbon.

Crowe, C. T., Troutt, T.R., and Chung, J.N., 1996, "Numerical Models for Two-Phase Turbulent Flows", *Annual Rev. Fluid Mech.*, Vol. 28, pp. 11-43.

Eaton, J. K., and Fessler, J. R., 1994, "Preferential Concentration of Particles by Turbulence", *Int. J. Multiphase Flow*, Vol. 20, pp. 169-209.

Hishida, K., Ando, A., and Maeda, M., 1992, "Experiments on Particle Dispersion in a Turbulent Mixing Layer", *Int. J. Multiphase Flow*, Vol 18, pp. 181-194.

Ishima, T., Hishida, K., and Maeda, M., 1993, "Effect of Particle Residence Time on Particle Dispersion in a Plane Mixing Layer", *ASME J. Fluids Engng.* Vol 115, pp. 751-759.

Issa, R. I., and Oliveira, P. J., 1994, "Numerical Predictions of Phase Separation in Two-Phase Flow Through T-Junctions", *Computers and Fluids*, Vol. 23, p. 347.

Issa, R.I., and Oliveira, P. J., 1995, "Numerical Prediction of Turbulence Dispersion in Two-Phase Jet Flows", In *Two-Phase Flow Modelling and Experimentation 1995*, Ed. G.P. Celata and R.K. Shah, Edizioni ETS, Italy, pp. 421-428.

Issa, R. I., and Oliveira, P. J., 1996, "Validation of Two-Fluid Model in Shear-Free Mixing Layers", *ASME FED* Vol 236, pp. 113-120.

Issa, R. I., and Oliveira, P. J., 1997, "Assessment of a Particle-Turbulence Interaction Model in Conjunction with an Eulerian Two-Phase Flow Formulation", In *Turbulence, Heat and Mass Transfer 2*, Eds. Hanjalic and Peeters, Delft University Press, pp. 113-120.

Oliveira, P.J., and Issa, R. I., 1994, "On the Numerical Treatment of Interphase Forces in Two-Phase Flow", *ASME-FED* Vol. 185, *Numerical Methods for Multiphase Flows*, pp. 131-140.

Pismen, L. M., and Nir, A., 1978, "On the motion of suspended particles in stationery homogeneous turbulence", *J. Fluid. Mech.*, Vol 84, pp. 193-206.

Reeks, M.W., 1977, "On the dispersion of small particles suspended in an isotropic turbulent field", *J. Fluid Mech.*, Vol. 83, pp. 529-546.

Simonin, O., Deutsch, E., and Minier, J. P., 1993, "Eulerian Predictions of the Fluid/Particle Correlated Motion in Turbulent Two-Phase Flows", *Applied Scientific Res.*, Vol. 51, pp. 275-283.

Wang, L-P., and Stock, D. E., 1993, "Dispersion of Heavy particles by Turbulent Motion", *J. Atmos. Sci.*, Vol. 50, pp. 1897-1913.